Supplement of

Addressing soil data needs and data-gaps in catchment scale environmental modelling: the European perspective

Brigitta Szabó et al.

* Correspondence: kassai.piroska@atk.hun-ren.hu (PK)

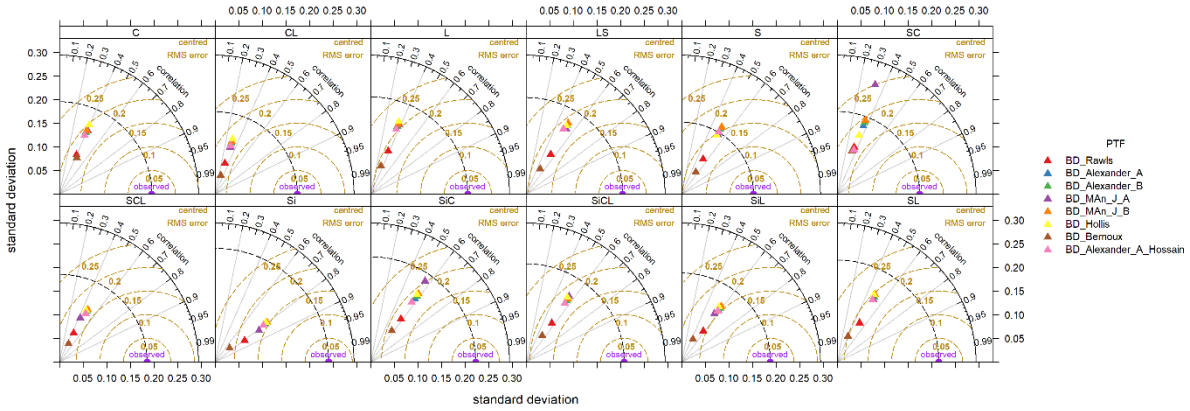

Figure S1. Taylor diagram, showing correspondence between the predicted and observed bulk density values by the applied pedotransfer functions, tested on point data in EU-HYDI dataset (N = 11,273) by soil texture classes, in terms of the correlation coefficient, the standard deviation and the centred root-mean-square error.

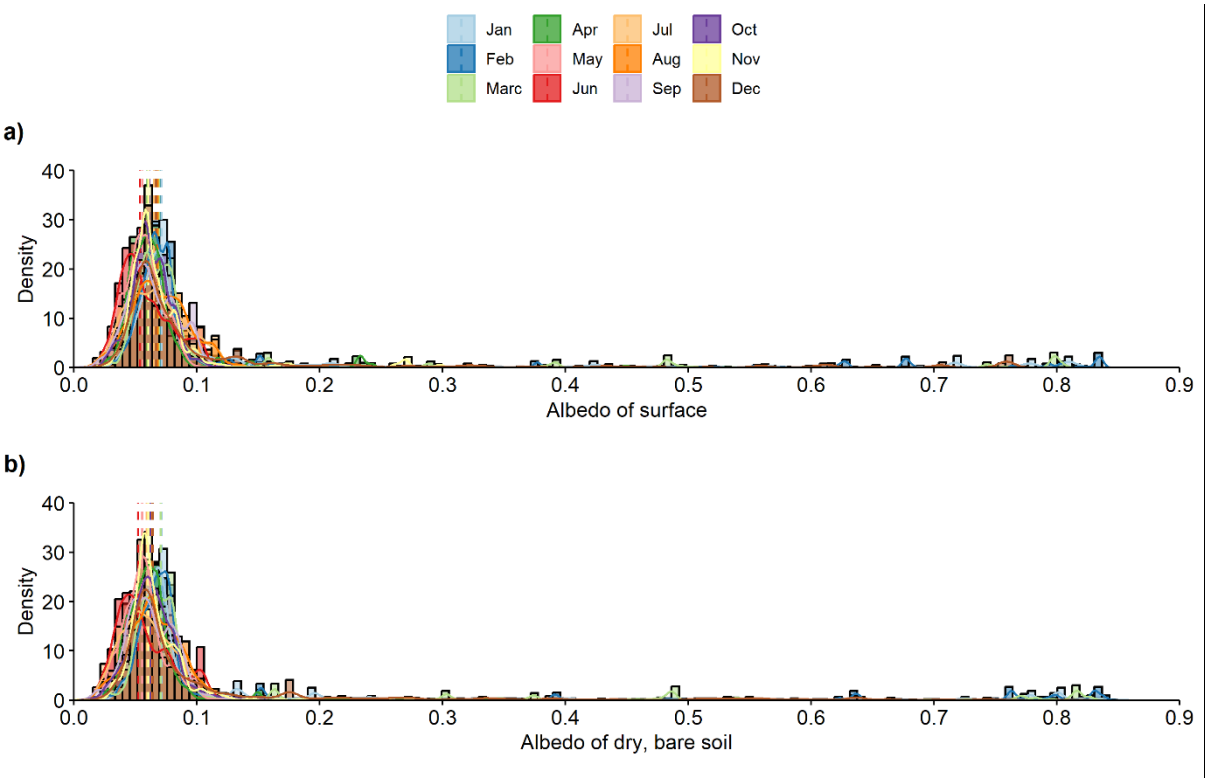

Figure S2. Histograms of the monthly surface and dry, bare soil albedo of year 2022 extracted from the MCD43A3 global database for the EU-HYDI topsoil layers (N = 1904). Vertical dashed lines indicate the median values.

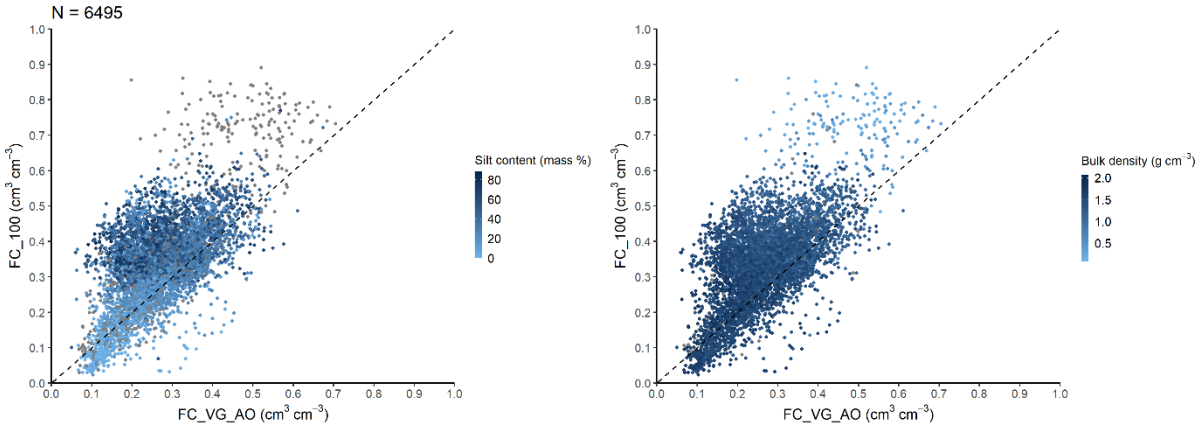

Figure S3. Scatterplot of internal drainage dynamics-based field capacity (FC_VG_AO) versus field capacity measured at -100 cm head with information on silt content and bulk density.

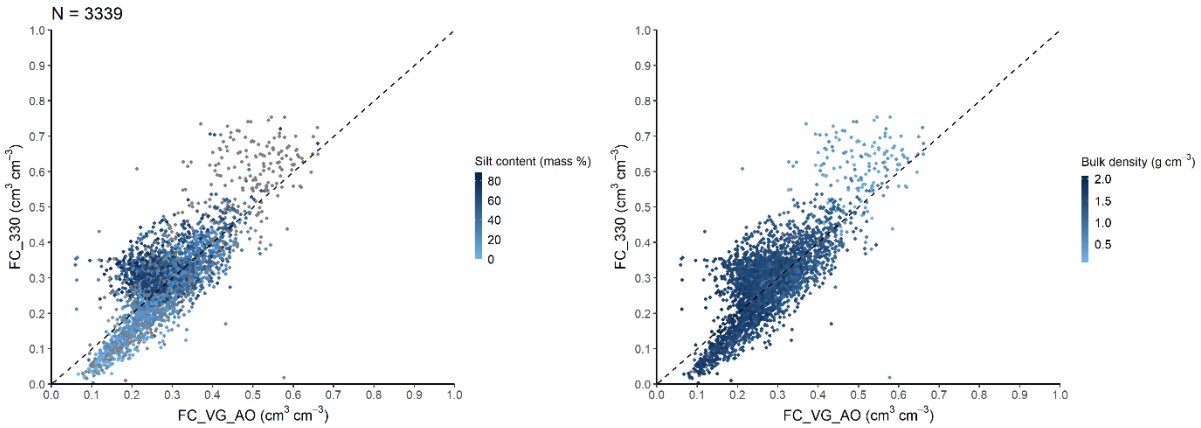

Figure S4. Scatterplot of internal drainage dynamics-based field capacity (FC_VG_AO) versus field capacity measured at -330 cm head with information on silt content and bulk density.

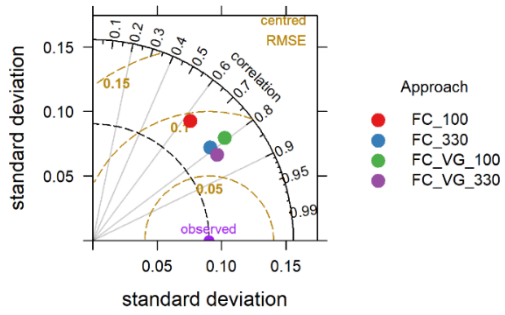

Figure S5. Taylor diagram showing correspondence between the differently defined field capacity values and the internal drainage dynamics-based field capacity (observed) values, analysed on the EU-HYDI dataset (N = 2,923), in terms of the correlation coefficient, the standard deviation and the centred root-mean-square error. FC_100, FC_300: measured FC at -100 and -330 matric potential, respectively; FC_VG_100, FC_VG_330: computed FC from the fitted VG model with parameter h (head) set at -100 and -330 cm matric potential, respectively.

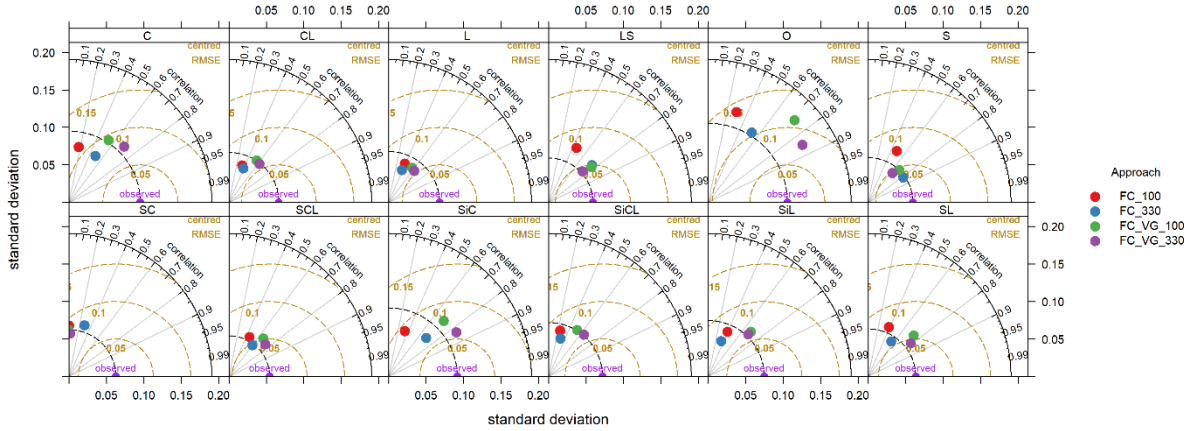

Figure S6. Taylor diagram showing correspondence between the internal drainage dynamics-based field capacity (observed) values and the differently defined field capacity values – measured at -100 and -330 matric potential and computed based on VG model with parameter h (head) set at -100 and -330 cm matric potential (FC_100, FC_330, FC_VG_100, FC_VG_330, respectively), tested on point data in EU-HYDI dataset (N = 2,923) by soil texture classes, in terms of the correlation coefficient, the standard deviation and the centred root-mean-square error. C: clays, CL: clay loams, L: loams, LS: loamy sands, O: organic soils, S: sands, SC: sandy clays, SCL: sandy clay loams, SiC: silty clays, SiCL: silty clay loams, SiL: silty loams, SL: sandy loams.

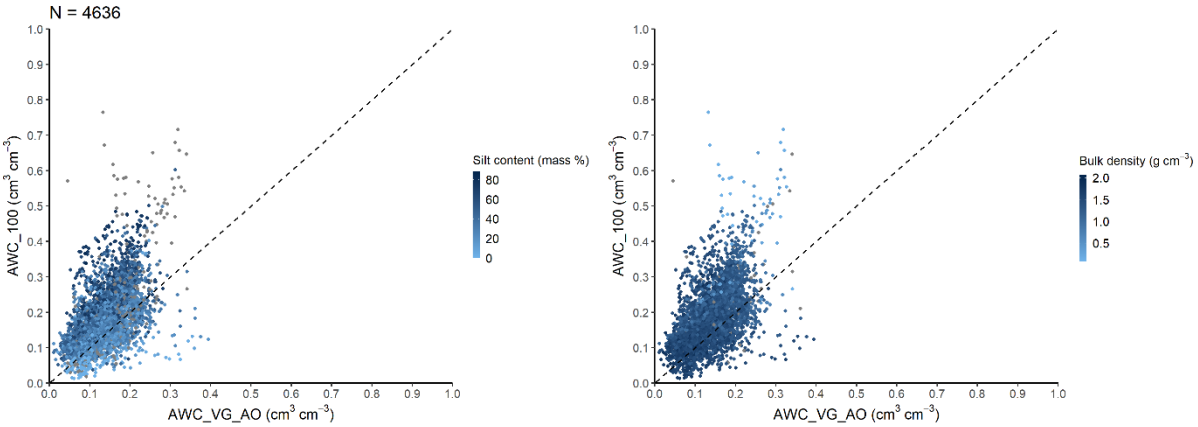

Figure S7. Scatterplot of available water capacity based on field capacity measured at -100 cm head and computed from the van Genuchten parameters with information on silt content and bulk density.

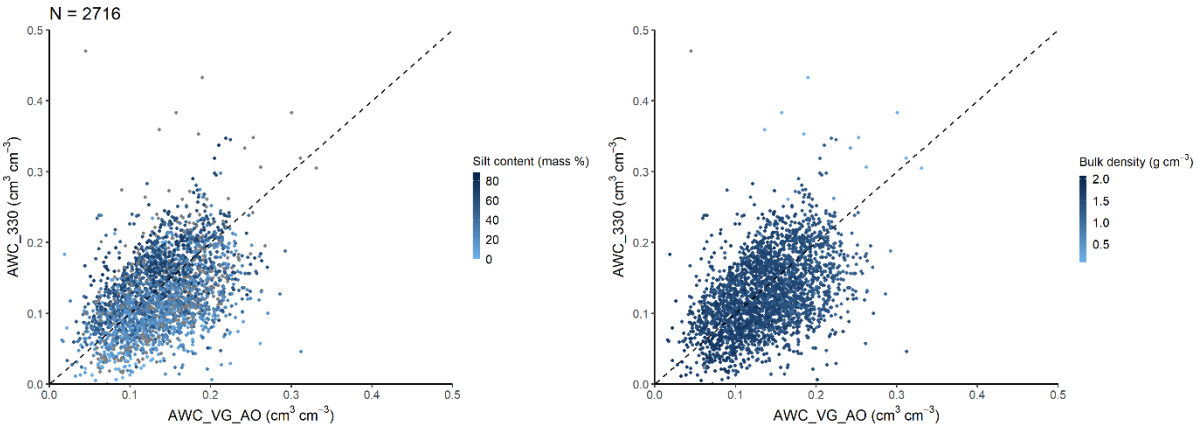

Figure S8. Scatterplot of available water capacity based on field capacity measured at -330 cm head and computed from the van Genuchten parameters with information on silt content and bulk density.

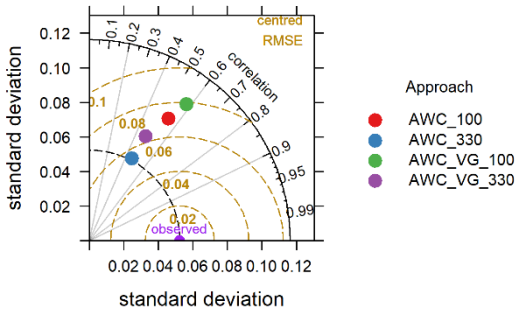

Figure S9. Taylor diagram showing correspondence between the available water capacity computed from internal drainage dynamics-based field capacity and wilting point derived based on VG parameters (observed) and differently defined available water capacity values, analysed on the EU-HYDI point dataset, in terms of the correlation coefficient, the standard deviation and the centred root-mean-square error. AWC_100, AWC_300: available water capacity computed from measured field capacity at-100 and -330 cm matric potential and wilting point, respectively (N = 4,213, N = 2379); AWC_VG_100, AWC_VG_330: available water capacity computed from field capacity at -100 and -330 cm matric potential and wilting point based on fitted VG parameters, respectively (N = 6602 for both).

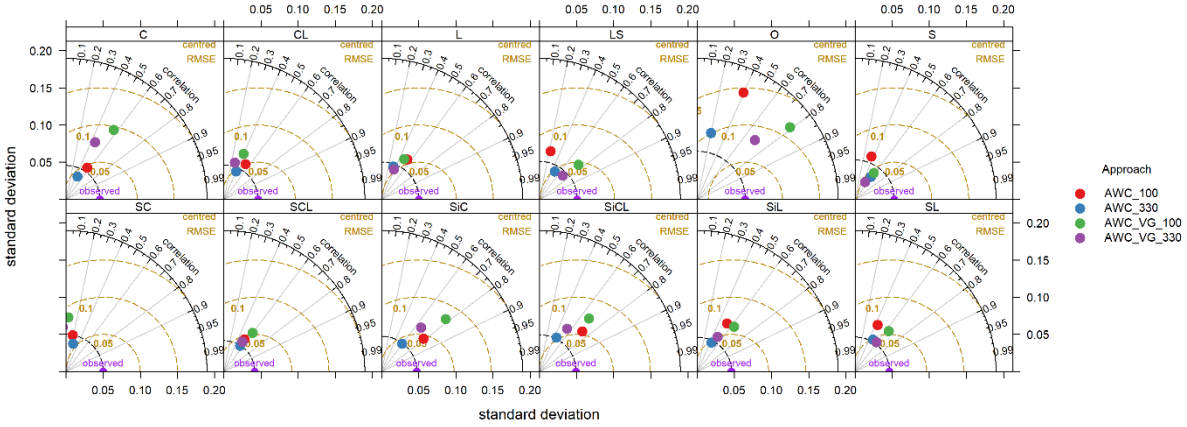

Figure S10. Taylor diagram showing correspondence between the differently computed available water capacity values – based on field capacity at -100 and -330 matric potential (N = 4,213, N = 2379) and computed based on VG model with parameter h (head) set at -100 and -330 cm matric potential (N = 6602 for both) to compute the field capacity (AWC_100, AWC_330, AWC_VG_100, AWC_VG_330, respectively) – and the internal drainage dynamics-based available water capacity (observed) values, tested on point data in EU-HYDI dataset by soil texture classes, in terms of the correlation coefficient, the standard deviation and the centred root-mean-square error. C: clays, CL: clay loams, L: loams, LS: loamy sands, O: organic soils, S: sands, SC: sandy clays, SCL: sandy clay loams, SiC: silty clays, SiCL: silty clay loams, SiL: silty loams, SL: sandy loams.